Palladium(II) Complexes of Oxybenziporphyrin

Marcin Stępień,[†] Lechosław Latos-Grażyński,*[,†] Timothy D. Lash,[‡] and Ludmiła Szterenberg[†]

Departments of Chemistry, University of Wrocław, 14 F. Joliot-Curie Street, Wrocław 50 383, Poland, and Illinois State University, Normal, Illinois 61761

Received April 13, 2001

8,19-Dimethyl-9,13,14,18-tetraethyloxybenziporphyrin coordinates palladium(II) to form the four-coordinate anionic complex $[(OBP)Pd^{II}]^-$. The NMR data provide evidence for the retention of macrocyclic aromaticity and coordination via a carbon σ-donor. Protonation of the external oxygen atom to give $[(HOBP)Pd^{II}]$ switches the molecule to a less aromatic phenol-like state, which is manifested by a significant reduction of the macrocyclic ring current. $[(AcOBP)Pd^{II}]$ and $[(TsOBP)Pd^{II}]$, two ester derivatives of $[(OBP)Pd^{II}]^-$, are similar to the protonated species, and their benzenoid character is more pronounced. However, reaction of $[(OBP)Pd^{II}]^-$ with methyl iodide leads to selective methylation of the coordinating C(22) atom to form a novel organopalladium complex $(OBPMe)Pd^{II}$. The strong shielding of the inner Me(22) ($\delta(^1H)$ −2.00 ppm in $CDCl_3$) indicates that the aromaticity of the macrocycle has been retained. At the same time the ^{13}C chemical shift of C(22) (44 ppm) shows that the palladium-bound carbon has undergone a drastic hybridization change. Alkylation with *n*-BuI yields a mixture of the O-substituted $[(n\text{-BuOBP})Pd^{II}]$ and the C-substituted $[(OBP\text{-}n\text{-Bu})Pd^{II}]$, which confirms the ambident nucleophilicity of $[(OBP)Pd^{II}]^-$. DFT calculations carried out for six tautomers of oxybenziporphyrin and the 22-methylated palladium species provide further insight into the electronic structure of the ligand and its complexes. Relative energies of the tautomers, increasing in the order [CH,NH,N,NH,O] < [CH,N,NH,N,OH] < [CH_2,N,NH,N,O] < [CH_2,N,N,N,OH], have been used to estimate the accessibility of four limiting delocalization modes postulated for oxybenziporphyrin and its derivatives. The state of macrocyclic aromaticity observed experimentally in the free base and the phenolic aromaticity of the O-protonated tautomer are the most favorable, and the latter has its energy higher by only 13 kcal/mol. The peculiar bonding situation in $(OBPMe)Pd^{II}$, which can be inferred from the NMR data, is also predicted by the DFT methods, which show a strongly distorted tetrahedral environment of C(22).

Introduction

Recently a novel group of porphyrin-like macrocycles has emerged, which can be generally classified as monocarbaporphyrinoids. Formally their formation requires a modification of the porphyrin skeleton that would provide a CH unit in place of one of the pyrrolenic nitrogens. Thus, the coordinating (CH,N,N,N) core becomes the denominator of this class of macrocycles.

By interchanging one of the nitrogens with a β-methine group of the same pyrrole, one transforms 5,10,15,20-tetraarylporphyrin ($TPPH_2$) into 2-aza-21-carba-5,10,15,20-tetraarylporphyrin (21-$CTPPH_2$, inverted porphyrin), which, while porphyrin-like in character, has fundamentally different electronic and coordination properties.[1−3] The peralkylated, *meso*-unsubstituted, inverted porphyrin ($CHAPH_2$) has been synthesized as well.[4,5] Taking advantage of the peculiar reactivity of nickel carbaporphyrin and free 21-carbaporphyrin, it was possible to generate their 2-*N*-methyl, 21-*C*-methyl, and 2-*N*-21-*C*-dimethyl derivatives.[6,7] Alternatively, the replacement of one pyrrole ring by benzene,[8] semiquinone,[9,10] cycloheptatriene,[11,12] indene,[11,13] azulene,[14] cyclopentadiene,[15] aliphatic bicyclic alkene,[16] or 2,4-linked thiophene[17] yielded a series of monocabaporphyrinoids.[18,19]

2-Aza-21-carba-23-oxaporphyrin, 2-aza-21-carba-23-thiaporphyrin, and 2-aza-21-carba-22-selenaporphyrin (i.e. "inverted" isomers of 21-oxaporphyrin, 21-thiaporphyrin, and 21-selenaporphyrin) combine features of both the inverted porphyrin and a 21-heteroporphyrin leading to a new type of coordination core

* To whom correspondence should be addressed.
[†] University of Wrocław.
[‡] Illinois State University.

(1) Chmielewski, P. J.; Latos-Grażyński, L.; Rachlewicz, K.; Głowiak, T. *Angew. Chem., Int. Ed. Eng.* **1994**, *33*, 779.
(2) Furuta, H.; Asano, T.; Ogawa, T. *J. Am. Chem. Soc.* **1994**, *116*, 767.
(3) Latos-Grażyński, L.Core Modified Heteroanalogues of Porphyrins and Metalloporphyrins. In *The Porphyrin Handbook*; Kadish, K. M., Smith, K. M., Guilard, R., Eds.; Academic Press: New York, 2000; Vol. 2, p 361.
(4) Liu, B. Y.; Brückner, C.; Dolphin, D. *Chem. Commun.* **1996**, 2141.
(5) Lash, T. D.; Richter, D. T.; Shiner, C. M. *J. Org. Chem*. **1999**, *64*, 7973.
(6) Chmielewski, P. J.; Latos-Grażyński, L. *J. Chem. Soc., Perkin Trans.2* **1995**, 503.
(7) Chmielewski, P. J., Latos-Grażyński, L.; Głowiak, T. *J. Am. Chem. Soc.* **1996**, *118*, 5690.
(8) Berlin, K.; Breitmaier, E. *Angew. Chem., Int. Ed. Engl.* **1994**, *33*, 1246.
(9) Lash, T. *Angew. Chem., Int. Ed. Engl.* **1995**, *34*, 2533.
(10) Lash, T. D. Chaney, S. T.; Richter, D. T. *J. Org. Chem*. **1998**, *63*, 9076.
(11) Berlin, K.; Steinbeck, C.; Breitmaier, E. *Synthesis* **1996**, 336.
(12) Lash, T. D.; Chaney, S. T. *Tetrahedron Lett.* **1996**, *37*, 8825.
(13) Lash, T. D.; Hayes, M. J. *Angew. Chem., Int. Ed. Engl.* **1997**, *355*, 841.
(14) Lash, T. D.; Chaney, S. T. *Angew. Chem., Int. Ed. Engl.* **1997**, *355*, 839.
(15) Berlin, K. *Angew. Chem., Int. Ed. Engl.* **1996**, *35*, 1820.
(16) Hayes, M. J.; Lash, T. D. *Chem. Eur. J.* **1998**, *4*, 508.
(17) Sprutta, N.; Latos-Grażyński, L. *Tetrahedron Lett.* **1999**, 8457.
(18) Lash, T. Syntheses of Novel Porphyrinoid Chromophores. In *The Porphyrin Handbook*; Kadish, K. M., Smith, K. M., Guilard, R., Eds.; Academic Press: New York, **2000**; Vol. 2, p 125.
(19) Lash, T. D. *Synlett.* **1999**, 279.

10.1021/ic010394a CCC: $20.00
Published on Web 11/27/2001

of the type (CH,N,X,N) with X = O, S^{20-22} or (CH, X, N, N) with X = Se.[23] The recent syntheses of dicarbaporphyrinoids and a doubly confused porphyrin have further extended the class of carbaporphyrinoid macrocycles.[24,25]

Inverted porphyrin and 21-methylated inverted porphyrin act as mono- or dianionic ligands for nickel(II) and nickel(III).[1,5,6,7,26,27] These macrocycles enforce the coordination of the pyrrolic sp^2 carbon to nickel(II).[1,5,6] In the case of (21-CH_3-CTPP)Ni^{II} the nickel(II) is four-coordinate with bonds to the three pyrrole nitrogens and the inner sp^3 carbon.[7] The methylated pyrrole is bound to the nickel via a pyramidal carbon forming a σ-bond. A similar mode of coordination can be expected in nickel(II) heptaalkyl inverted porphyrin $[(CHAPH)Ni^{II}]^+$ and $[2\text{-N-}CH_3CTPPH)Ni^{II}]^+$ protonated at the C(21) carbon.[5,28]

In the paramagnetic (2-NCH_3-21-CH_3CTPP)Ni^{II}I the methylated pyrrole is linked to nickel in the η^1-fashion but the coordinating C(21) carbon preserves the features related to the trigonal sp^2 hybridization.[7] Addition of the phenyl Grignard reagent to a toluene solution of the nickel(II) chloride complex of dimethylated inverted porphyrin (2-NCH_3-21-CH_3CTPP)Ni^{II}-Cl gave a rare paramagnetic (σ-phenyl)nickel(II) species (2-NCH_3-21-CH_3CTPP)Ni^{II}Ph which contains simultaneously equatorial and apical Ni^{II}−carbon bonds.[27] The inverted porphyrins and their methylated derivatives stabilize the unusual organocopper(II) complexes (CTPP)Cu^{II}, (2-NCH_3CTPP)Cu^{II}, (CTPPH)Cu^{II}X, (2-NCH_3CTPPH)Cu^{II}X (X: Cl^-, TFA^-), and [(2-NCH_3-21-CH_3CTPP)Cu^{II}Cl.[28] Recently Furuta and co-workers have demonstrated that inverted porphyrin acts as a trianionic ligand stabilizing silver(III).[29] This brief overview demonstrates that until now the coordination chemistry of monocarbaporphyrinoids has been narrowed to the derivatives of inverted porphyrin.

The development of polydentate ligands with a potential carbon donor favorably oriented toward the transition metal ion offers a new general strategy to stabilize untypical oxidation states and coordination geometries in organometallic compounds.[30−35] The metal−carbon bond can be firmly held in the cavity of such a ligand so that the possible dissociation of the M−C bond will be impaired. In light of these we have decided to probe the coordination chemistry of carbaporphyrinoid macrocycles other than inverted porphyrins. Here we present our results on the coordination properties of 8,19-dimethyl-9,13,14,18-tetraethyloxybenziporphyrin $(OBPH)H_2$ (**1**). From now on we will use the symbol OBP to denote the hypothetical trianion obtained from the free base by abstraction of the two pyrrolic protons and the C-bound proton H(22). The groups attached to the O(2) atom will be indicated by a prefix (e.g. AcOBP for *O*-acetyl derivative), while those bound to C(22) will appear as suffixes (OBPMe for 22-methylation).

Chart 1

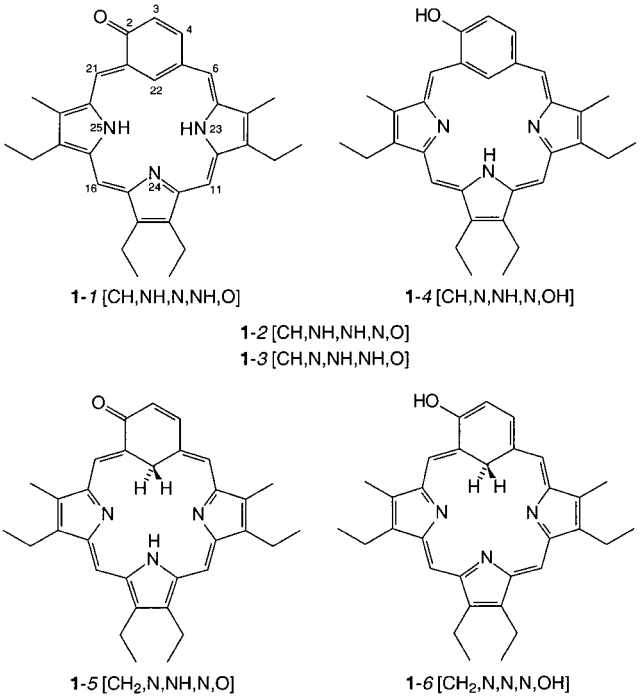

Oxybenziporphyrin is conceptually derived from benziporphyrin,[8,10] in which a benzene ring replaces one of the porphyrinic pyrroles leading to a structure devoid of macrocyclic aromaticity. However, 2-hydroxybenzoporphyrin **1**-*4* is found to exist solely as its keto form **1**-*1*−*3* (oxybenziporphyrin), in which the 18e porphyrinoid π-delocalization pathway is restored (Chart 1).[9,10] The hypothetical forms **1**-*5* and **1**-*6* will be of significance in further discussion.

To explore the coordination of metal ions by oxybenziporphyrin we decided to focus on the chemistry of palladium(II). A variety of palladium(II) complexes with porphyrins,[36] heteroporphyrins,[37] and doubly-N-confused porphyrins[25] have been isolated and characterized. Importantly, the palladium(II) ion is susceptible to phenyl coordination in a cyclopalladation process.[38−40] Once the carbon donor is built into macrocylic or pincer ligands, the palladium(II) ion forms robust organometallic compounds.[30−32,35,38,41] These species, while sufficiently inert, form more readily that their Pt(II) congeners.

Here we report on the synthesis and spectroscopic properties of oxybenziporphyrin complexes with Pd(II). In particular we

(20) Heo, P.-Y.; Shin, K.; Lee, C.-H. *Tetrahedron Lett.* **1996**, *37*, 197.
(21) Lee, C.-H. Kim, H.-J. *Tetrahedron Lett.* **1997**, *38*, 3935.
(22) Lee, C.-H.; Kim, H.-J.; Yoo, D.-W. *Bull. Korean Chem. Soc.* **1999**, *20*, 276.
(23) Pacholska, E.; Latos-Grażyński, L.; Szterenberg, L.; Ciunik, Z. *J. Org. Chem.* **2000**, *65*, 8188.
(24) Lash, T. D.; Romanic, J. L.; Hayes, M. J.; Spence, J. D. *Chem. Commun.* **1999**, 819.
(25) Furuta, H.; Maeda, H.; Osuka, A. Yasutake, M.; Shinmyozu, T.; Ishikawa Y. *Chem. Comun.* **2000**, 1143.
(26) Chmielewski, P. J.; Latos-Grażyński, L. *Inorg. Chem.* **1997**, *36*, 840.
(27) Chmielewski, P. J.; Latos-Grażyński, L. *Inorg. Chem.* **2000**, *39*, 5639.
(28) Chmielewski, P. J.; Latos-Grażyński, L, Schmidt, I. *Inorg. Chem.* **2000**, *39*, 5475.
(29) Furuta, H.; Ogawa, T.; Uwatoko, Y.; Araki, K. *Inorg. Chem.* **1999**, *38*, 2676.
(30) van Koten, G. *Pure Appl. Chem.* **1989**, *61*, 1681.
(31) Rietveld, M. H. P.; Grove, D. M.; Van Koten, G. *New. J. Chem.* **1997**, *21*, 751.
(32) Gossage, R. A.; van de Kuil, L. A.; van Koten, G. *Acc. Chem. Res.* **1998**, *31*, 423.
(33) Gozin, M.; Weisman, A.; Ben-David, Y.; Milstein, D. *Nature* **1993**, *364*, 699.
(34) Newkome, G. R.; Puckett, W. E.; Gupta, V. K.; V. K.; Kiefer, G. E. *Chem. Rev.* **1986**, *86*, 451.
(35) Giesbrecht, G. R.; Hanan, G. S.; Kickham, J. E.; Loeb, S. J. *Inorg. Chem.* **1992**, *31*, 3286.
(36) Stolzenberg, A. M.; Schussel, L. J.; Summers, J. S.; Foxman, B. M.; Petersen, J. L. *Inorg. Chem.* **1992**, *31*, 1678.
(37) Latos-Grażyński, L.; Lisowski, J.; Chmielewski, P. J.; Grzeszczuk, M.; Olmstead, M. M.; Balch, A. L. *Inorg. Chem.* **1994**, *33*, 192.
(38) Steenwinkel, P.; Gossage, R. A.; Grove, D. M.; van Koten, G. *Chem. Eur. J.* **1998**, *4*, 759.
(39) Steenwinkel, P.; Gossage, R. A.; Maunula, T.; Grove, D. M.; van Koten, G. *Chem. Eur. J.* **1998**, *4*, 763.
(40) Jolliet, P.; Gianini, M.; von Zelewsky, A.; Bernardinelli, G.; Stoeckli-Evans, H. *Inorg. Chem.* **1996**, *35*, 4883.
(41) van der Boom, M.; Liou, S.-Y.; Ben-David, Y.; Shimon, L. J. W.; Milstein, D. *J. Am. Chem. Soc.* **1998**, *120*, 6531.

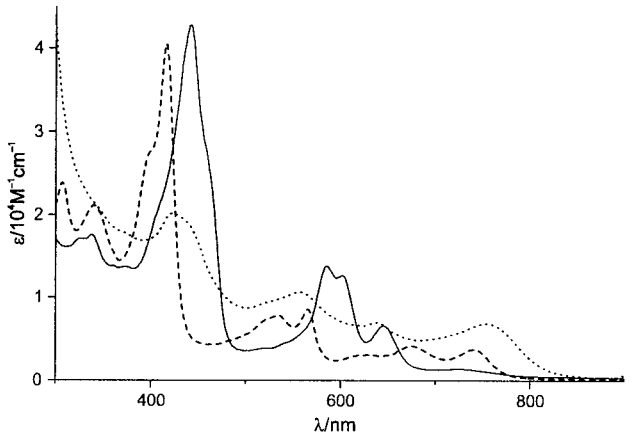

Figure 1. Electronic spectra of **2** (—), **3** (---), and **5** (···, excess MeI present) recorded at 298 K in MeCN.

Scheme 1

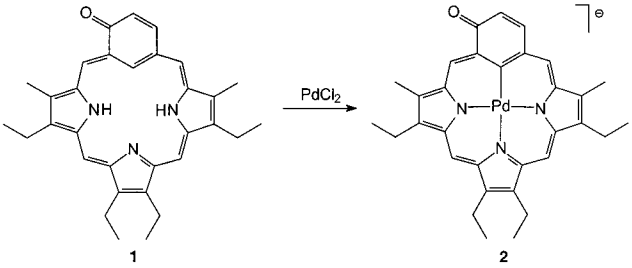

have focused on the effects of complexation and electrophile addition on the aromaticity of the ligand.

Results and Discussion

Formation and Characterization of K[(OBP)Pd^{II}]. Reaction of palladium(II) chloride with oxybenziporphyrin (**1**) in acetonitrile in the presence of anhydrous K_2CO_3 results in the formation of the four-coordinate K[(OBP)Pd^{II}] (**2**) in 96% yield (Scheme 1). Potassium carbonate neutralizes HCl formed in the course of insertion and provides the necessary countercation to balance the charge of the anionic [(OBP)Pd^{II}]$^-$. It is important that the stoichiometric amount of metal carrier be used for the reaction. The product obtained in the presence of excess $PdCl_2$ quickly loses solubility after removal of the solvent and has not been characterized. Probably the insertion process is followed by coordination of palladium to the phenolic oxygen and the resultant species oligomerize in the solid state.

The electronic absorption spectrum of K[(OBP)Pd^{II}] (**2**) (Figure 1) with its intense Soret-like band (443 nm in MeCN) and a set of bands in the Q region is similar to the spectrum of the free ligand.[9,10] The spectrum is slightly solvent-dependent.

The ^{1}H NMR spectrum of K[(OBP)Pd^{II}] resembles that of (OBPH)H_2 (Figure 2).[9,10] The complete assignment of all resonances (trace A, Figure 2) has been obtained from COSY and NOESY experiments. For the sake of comparison we have carried out parallel 2D experiments for (OBPH)H_2 to confirm that both patterns in the 10−7 ppm regions are alike. The most notable feature of **2** is coordination of palladium(II) in the plane of the C_6 ring through the unprotonated trigonally hybridized carbon(22) center. The H(22) resonance of (OBPH)H_2, located at −7.2 ppm, is absent in the ^{1}H NMR spectrum of **2,** and consequently, the H(4) signal, which in **1** shows couplings to H(3) and H(22), simplifies to a doublet. Partial assignment of ^{13}C resonances has been carried out using ^{1}H−^{13}C correlation techniques (HMQC, HMBC). The chemical shift found for C(2)

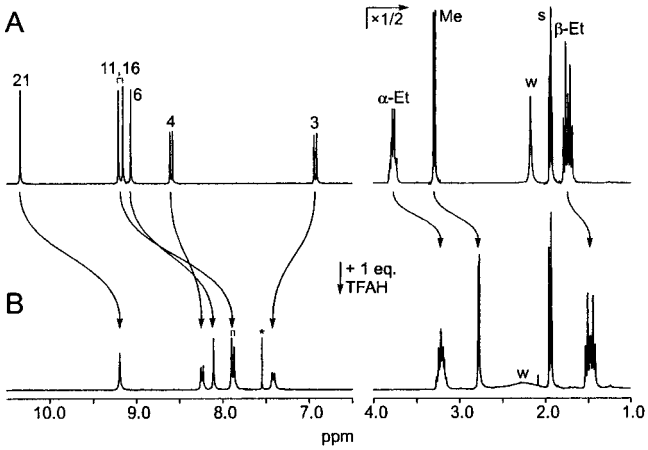

Figure 2. ^{1}H NMR spectrum of **2** (298 K, MeCN-d_3, trace A) and **3** (trace B, same conditions, obtained by addition of 1 equiv of TFAH to the sample).

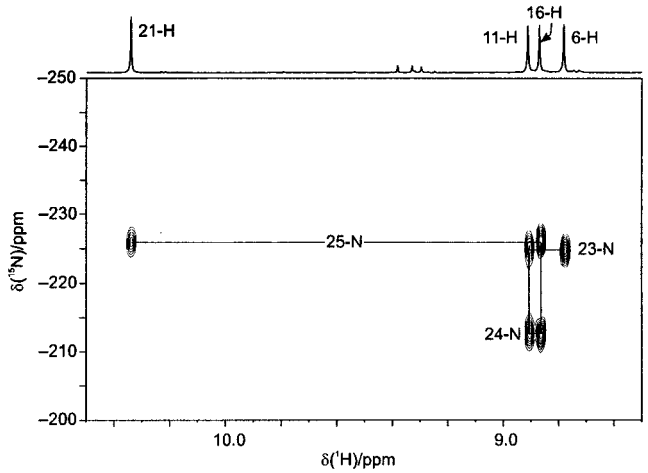

Figure 3. ^{1}H−^{15}N correlation spectrum of **2** (298 K, $CDCl_3$). The solid line indicates the connectivity within the H_{meso}−N coupling network.

(191 ppm) is fairly typical of a carbonyl fragment, while the C(22) resonance, located at 139 ppm, is indicative of the sp^2 hybridization. The ^{1}H−^{15}N HMQC experiment performed for **2** (Figure 3) provides an unambiguous assignment of the coordinating nitrogens and, in addition, of the *meso* protons. ^{15}N chemical shifts measured for **2** are in the range found for porphyrins and their complexes (from −126 to −263 ppm).[42] Thus, the NMR data provide evidence for the coordination of the aromatic trianionic ligand derived from **1** after the dissociation of two NH protons and one CH proton.

Protonation of K[(OBP)Pd^{II}]. Addition of 1 equiv of TFAH to the solution of **2** in acetonitrile transforms the green anion [(OBP)Pd^{II}]$^-$ into its red-violet protonated form (HOBP)Pd^{II} (**3**) (Scheme 2). Titration followed by UV−vis spectroscopy proceeds with well-defined isosbestic points, and the final spectrum of **3** is shown in Figure 1. The strong Soret band shifts hypsochromically to 416 nm but is retained. This remains in striking contrast with the spectrum of the O-protonated dication (HOBPH)H_3^{2+}, whose broadened features were explained in terms of the loss of aromaticity.[9,10,18] The phenolic moiety, which in the case of **3** is held in the macrocyclic plane by the coordinated metal atom, is conjugated with the tripyrrolic subunit more strongly than in (HOBPH)H_3^{2+}, where it may be

(42) Medforth, C. NMR Spectroscopy of Diamagnetic Porphyrins. In *The Porphyrin Handbook*; Kadish, K. M., Smith, K. M., Guilard, R., Eds.; Academic Press: New York, 2000; Vol. 5, p 1.

Scheme 2

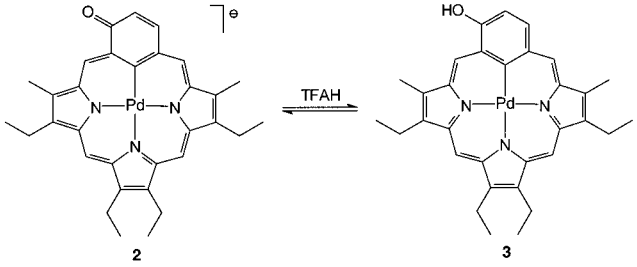

Scheme 3

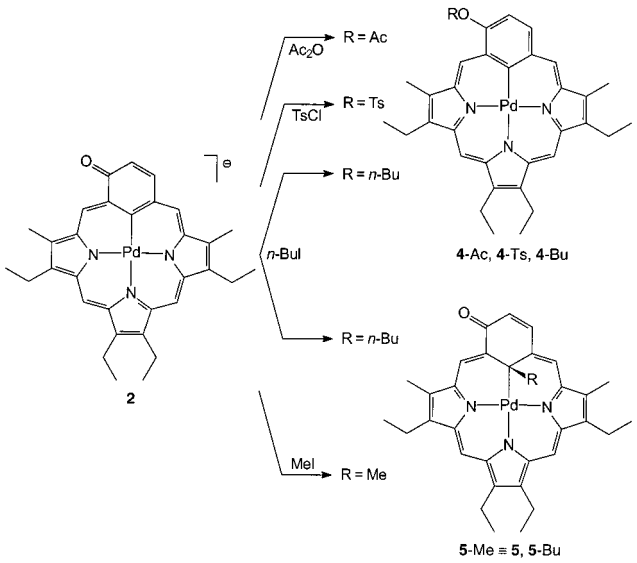

tilted out of the macrocyclic plane. Stirring the solution of **3** with anhydrous K_2CO_3 regenerates the anion. However, when dissolved in pyridine, **3** does not undergo deprotonation, which sets the other limit of its acidity.

The result of an ^{1}H NMR spectroscopic titration carried out by addition of TFAH to a solution of **2** in acetonitrile-d_3 at 293 K is shown in Figure 2 (trace B). Under these conditions proton exchange rates involving **2** and **3** are fast on the NMR time scale and consequently only a smooth change of the chemical shifts can be observed in the whole titration range. Addition of more than 1 equiv of TFAH does not cause further changes in the spectrum apart from progressive broadening of the signals. The macrocyclic ring current effect is markedly reduced in **3** as can be inferred from the more upfield shifts of the meso and alkyl resonances. The effect of protonation upon the positions of signals H(3) and H(4) is certainly more complex, presumably involving the diamagnetic current induced in the six-membered ring as well as a change in the anisotropy of the C−O bond.

Cyclic voltammetry of K[(OBP)Pd^{II}] in acetonitrile solution shows a reversible oxidation at 0.32 V (vs AgCl/Ag). For (HOBP)Pd^{II} the oxidation wave shifts to 0.43 V.

Esterification of K[(OBP)Pd^{II}]. In contrast with the free base, known to be fairly unreactive,[10] [(OBP)Pd^{II}]$^-$ readily reacts with a variety of electrophiles. Application of two typical esterification reagents, acetic anhydride or *p*-toluenesulfonyl chloride, yielded the respective ester derivatives of palladium(II) hydroxybenziporphyrin (**3**), i.e., (AcOBP)Pd^{II} and (TsOBP)Pd^{II} (**4**-Ac and **4**-Ts, Scheme 3), whose electronic spectra are almost identical with the spectrum of **3**. The changes observed in their ^{1}H NMR spectra follow the pattern already described for **3**, although the general upfield trend is now more pronounced. ^{13}C chemical shifts of C(22) and C(2) in **4**-Ac are 142 and 156 ppm, respectively.

Alkylation of K[(OBP)Pd^{II}]. Of particular importance is the observation that **2** is susceptible to methylation at the C(22) atom. Thus, [(OBP)Pd^{II}]$^-$ rapidly reacts with methyl iodide to yield a novel organopalladium(II) complex (OBPMe)Pd^{II} (**5**, Scheme 3). Judging by the ^{1}H NMR spectrum of the reaction mixture, the process is nearly quantitative. Such a reactivity resembles that of (CTPP)Ni^{II}, (2-NCH$_3$CTPP)Ni^{II}, and (2-NCH$_3$-CTPP)Cu^{II} and C-methylation of *trans*-2,6-bis[(dimethylamino)-methyl]phenyl-*N*,*C*,*N*′ complex of platinum(II), [PtI(C$_6$H$_3$-(CH$_2$NMe$_2$)$_2$-*o*,*o*′)]$^+$.[7,28,43]

The electronic absorption spectrum of **5** is broadened and less intense compared to the spectra of **2** or **3** (Figure 1), which might indicate that the aromaticity of the macrocycle is disrupted upon methylation. Contrarily, the ^{1}H NMR spectrum of **5** indicates the presence of a strong aromatic ring current (Figure 4, trace A). Thus, the meso resonances are detected practically in the same positions as those of **2**. However, the H(3) and H(4) signals are displaced further downfield, by 0.8 and 0.3 ppm, respectively. The Me(22) group gives rise to a singlet at −2.00 ppm ($CDCl_3$), which shows dipolar couplings to H(6) and H(21) in the NOESY map. This upfield shift is diagnostic for methyl groups located in the center of aromatic macrocycles as found for diamagnetic *N*-methyl porphyrins[44] and particularly for 21-C-methylated inverted porphyrins and their complexes (21-CH$_3$-CTPPH$_2$, −4.84 ppm; 2-NCH$_3$-21-CH$_3$CTPPH, 1.58 ppm; (21-CH$_3$CTPP)Ni^{II}, −3.15 ppm).[7] The ^{13}C chemical shift of C(22) is 44 ppm (98 ppm upfield with respect to **2**), which can only be rationalized by assuming a pesudotetrahedral geometry at this carbon atom. C(2) resonates at 184.3 ppm, which corresponds to a carbonyl group.

The macrocyclic aromaticity observed in **5** is apparently at variance with the assumed simultaneous presence of an sp^3 center and a carbonyl unit, both of which put an obstacle in the delocalization pathways. This problem will be discussed later in conjunction with DFT calculations.

Systematic titration of **5** with TFAH monitored by ^{1}H NMR results in a smooth although relatively small increase of the chemical shifts, so the effect of protonation on aromaticity is moderate. The difference between the shifts of H(3) and H(4) is reduced, and almost certainly proton addition takes place at the O(2) atom. Surprisingly, after addition of more than 1 equiv of acid the signals begin to move in the reverse direction, i.e., upfield. Possibly TFAH associates to **5**-H$^+$ through hydrogen bonding although coordination to palladium cannot be ruled out.

The selectivity of the alkylation reaction heavily depends on the alkylating agent being used. *n*-Butyl iodide produces a roughly equimolar mixture of the O(2)- and C(22)-butylated species, **4**-Bu and **5**-Bu, respectively. Their spectral characteristics compare well with those of other O- and C-substituted derivatives **4**-R and **5**-R (the ^{1}H NMR spectrum of **4**-Bu is shown in Figure 4, trace B). An additional feature seen in the ^{1}H NMR spectrum of **5**-Bu is the diastereotopic differentiation of the 22-Bu methylene resonances (especially strong for the α-Bu signal, Figure 4, trace C). This reflects the fact that addition to C(22) removes the unique symmetry plane of the macrocycle. Accordingly, all species **5**-R are chiral in a similar way as described for complexes of *N*-methylporphyrins and carbaporphyrin.[7,45] The behavior of butyl iodide shows that there

(43) Grove, D. M.; van Koten, G.; Louwen, J. N.; Noltes, J. G.; Spek, A. L.; Ubbels, H. J. C. *J. Am. Chem. Soc.* **1982**, *104*, 6609.
(44) Lavallee, D. K. *The Chemistry and Biochemistry of N-substituted Porphyrins*; VCH Publishers: New York, 1987.

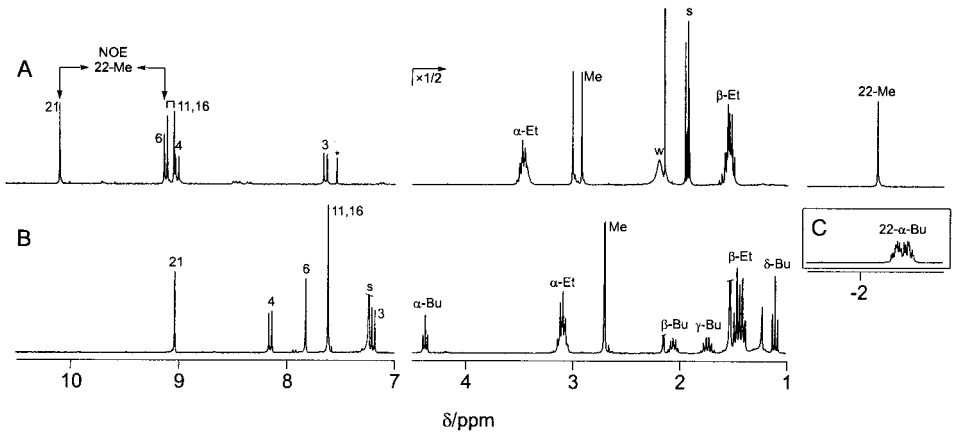

Figure 4. ^{1}H NMR spectra of **5**-Me (298 K, MeCN-d_3, trace A) and **4**-Bu (298 K, $CDCl_3$, trace B). Trace C shows the 22-α-Bu signal of **5**-Bu.

Table 1. Feasible Delocalization Modes within the Six-Membered Ring of Oxybenziporphyrin and Its Complexes

	Y =	R =	R' =	
A	H			**1**-*1,2,3*
	Pd			**2**
	Me			**5**
B	H	H		**1**-*4*; **1**-H_2^{2+}
	Pd	H		**3**
	Pd	Ac,Ts, *n*-Bu		**4**-Ac,Ts,Bu
	Me	H		**5**-H^+
C	H		H	**1**-*5*
	Pd		Me	**5**
D	H	H	H	**1**-*6*
	Pd	H	Me	**5**-H^+

is no sharp distinction between the O- and C-nucleophilicity of **2**, and the selectivity of different electrophiles may depend on both their steric demands and electronic characteristics (such as polarizability[46]).

Tautomers of (OBPH)H_2. DFT Calculations. It could be seen from the preceding discussion that appropriate substitution of atoms O(2) and C(22) can strongly influence the electronic structure of oxybenziporphyrin and its complexes. Crucial in this respect are the properties of the C_6O unit, which participates in the macrocyclic delocalization in a manner determined by the internal/external substitution pattern. In principle, four limiting delocalization routes can be distinguished, as shown in Table 1. States **A** and **D**, with the conjugation pathways passing respectively through the C(22) atom and around it, will contribute to the macrocyclic aromaticity. On the other hand, state **B**, known to prevail in the 2-unsubstituted benziporphyrin,[8] will favor the [6]annulene aromaticity, while state **C**, in which a keto function and an sp^3 carbon are simultaneously present, disables all delocalization routes involving the C_6O fragment.

As indicated in Table 1, for certain of the species **1**−**5** several delocalization states are potentially accessible. For instance states **A** and **C** may be required to describe the 22-alkylated complex **5** to account for the macrocyclic aromaticity (**A**) and the tetrahedral C(22) atom (**C**). Moreover charge-separated contributions of type **B** can accompany state **A** and, by analogy, there may be **D**-type admixtures present in **C** (Chart 2).

Obviously the electronic structure of (OBPH)H_2 and its derivatives cannot be unraveled in terms of **A**−**D** relying solely on the quantitative information provided by NMR. One can note, however, that each of tautomers **1**-*1*−*6* is a realization of some C(22)/O(2) substitution pattern and thus may closely approach the limit of the corresponding delocalization state. Therefore a theoretical treatment of the tautomers of **1** may provide additional insight into the feasibility of states **A**−**D**.

To estimate the relative stability of the six tautomers we have applied the density functional theory (DFT) in a similar way as previously described for inverted porphyrins, sapphyrin, diheterosapphyrins, and inverted selenaporphyrin.[23,47−49] DFT methods and high-level ab initio calculations have recently been applied to porphyrins, porphyrin isomers, metalloporphyrins, and related systems.[47−52] These theoretical investigations addressed problems of molecular geometry, NH tautomerization, electronic spectra, and effects of substitution on electronic structure.

The optimized geometries of the representative tautomers of **1′** (**1** with peripheral alkyls replaced by hydrogens) and the corresponding relative energies (B3LYP/6-31G**//B3LYP/6−31*G) are shown in Figure 5. In each case the macrocycle remains virtually planar irrespective of the protonation state. Root-mean-square deviations of bond lengths along the three predicted delocalization pathways are given for the relevant tautomers in Table 2. Inspection of these values leads to the conclusion that the postulated delocalization modes **A**−**D** are indeed realized by the theoretical model. In **1′**-*1* and **1′**-*6* the two types of macrocyclic aromaticity **A** and **D** are present, as indicated by the C−C distances along the respective delocalization paths (21−1−22−5−6 and 21−1−2−3−4−5−6), which approach the value of 1.40 Å. In **1′**-*5* localization of double bonds can be seen, which agrees with the assumed state **C**. Interestingly, bond lengths within the C_6 ring of tautomer **1′**-*4* do not completely average out. It is conceivable that the presence of the 2-hydroxyl substituent suffices to impart some **A**-type aromatic character to the basically benzene-like structure.

(45) Kubo, H.; Aida, T.; Inoue, S.; Okamoto, Y. *Chem. Comun.* **1988**, 1015.
(46) March, J. *Advanced Organic Chemistry*, 4th ed.; Wiley and Sons: New York, 1992; pp 365−368.
(47) Szterenberg, L.; Latos-Grażyński, L. *Inorg. Chem.* **1997**, *36*, 6291.
(48) Szterenberg, L.; Latos-Grażyński, *J. Phys. Chem. A* **1999**, *103*, 3302.
(49) Szterenberg, L.; Latos-Grażyński, L. *THEOCHEM* **1999**, *490*, 33.
(50) Ghosh, A. Quantum Chemical Studies of Molecular Structures and Potential Energy Surfaces of Porphyrins and Hemes. In *The Porphyrin Handbook*; Kadish, K. M., Smith, K. M., Guilard, R., Eds.; Academic Press: New York, 2000; Vol. 7, p 1.
(51) Ghosh, A. *Angew. Chem., Int. Ed. Engl.* **1995**, *34*, 1028.
(52) Vanber, T.; Ghosh, A. *J. Am. Chem. Soc.* **1999**, *121*, 12154.

Chart 2

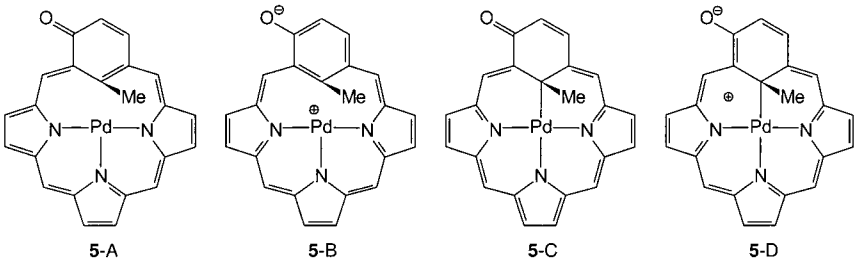

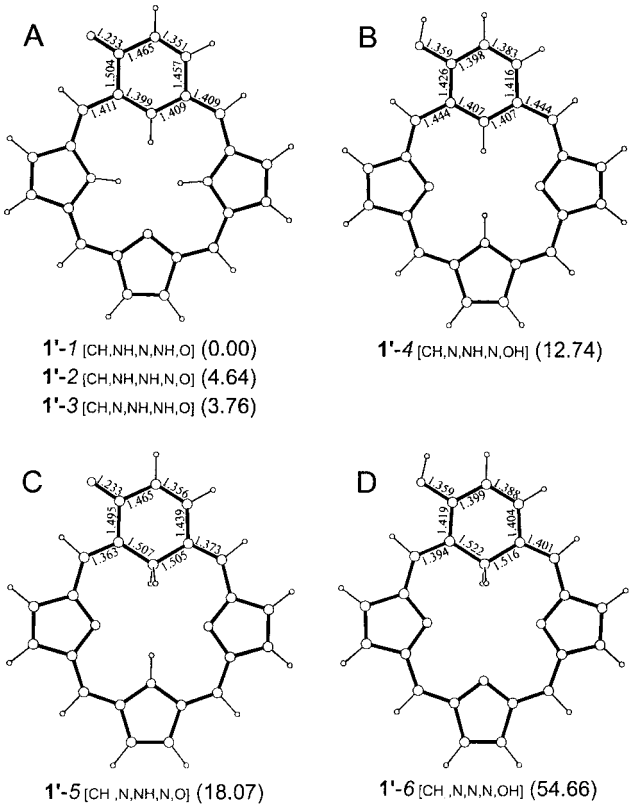

Figure 5. DFT-optimized structures of **1′**-*1*−*6* (relative energies in kcal/mol). The relevant bond distances are given in Å.

The bond distances within the tripyrrolic framework (given in the Supporting Information) indicate that this part of the macrocycle is highly conjugated in all the forms **1**-*1*−*6*. In all cases they are comparable to the corresponding distances calculated for porphine and inverted porphine.[47] In **1**-*5* and **1**-*6* the C(22) atom shows a slight distortion from the perfect tetrahedral geometry. The expanded C(1)−C(22)−C(5) angle (117° in **1**-*5* and 116° in **1**-*6*) and the compressed H−C(22)−H (102 and 100°, respectively) indicate that the macrocyclic framework imposes certain strain on the 22-methylene moiety.

Comparison of the energy values calculated for **1′**-*1*−*3* shows that, as expected, they are the most stable tautomers and the effect of reshuffling the NH protons does not exceed 5 kcal/mol. The energies obtained for **1′**-*4* and **1′**-*5* are slightly higher than those determined for **A**-type tautomers but still within acceptable limits. The calculations suggest that the **D**-type delocalization, exemplified by **1′**-*6*, will be relatively disfavored. However, modes **B** and **C** should be considered seriously whenever they may contribute to the electronic structure. Finally it should be noted that repulsion between the protons inside the macrocyclic core, which varies from tautomer to tautomer, also affects the predicted energy gaps (cf. the energy difference between the cis and trans tautomers of porphyrin, for which a value of 6−11 kcal/mol was calculated).[53,54]

The energy differences obtained for the tautomers provide a tentative measure of the π-electron effects caused by the redistribution of protons among the potentially nucleophilic sites in **1**, showing that they are generally small. It is reasonable to expect that these effects should be of comparable magnitude in metal complexes of oxybenziporphyrin even in the presence of back-donation, which in the case of Pd(II) interferes with the π-system of the ligand.

The analysis of the calculated relative stability of oxybenziporphyrin tautomers may provide additional insight into the coordinating properties of oxybenziporphyrin. Considering the mechanism of metal ion insertion into the coordination core of inverted porphyrin, we included a preorganization step into the mechanistic route.[47] To satisfy the requirements imposed by the inserted metal ion the molecular and electronic structures of the ligand have to be prearranged. A preorganization may contribute to the overall activation energy of metal insertion. Energies of preorganization for **1′**-*1* → **1′**-*4* (12.74 kcal/mol, oxybenziporphyrin → 2-hydroxybenziporphyrin) and **1′**-*1* → **1′**-*5* (18.07 kcal/mol, change in hybridization of C(22)) are comparable with activation energies determined for metal ion insertion to porphyrins and *N*-methylporphrins.[55−58] However, mechanistic factors that influence the value of activation enthalpy may be essentially different for regular porphyrins and oxybenziporphyrin. The relatively small calculated ligand preorganization energy leads to an expectation that oxybenziporphyrin will coordinate using several different coordination modes depending on peripheral modifications and, presumably, on the nature of the central atom. The very large energy difference between **1**-*1* and **1**-*6* (54.66 kcal/mol) excludes the contribution of **1**-*6* in tautomeric equilibria of oxybenziporphyrin. However, as shown experimentally, once the palladium(II) ion binds to the three pyrrolic nitrogen atoms, both coordination modes of the C(22) atom (trigonal and tetrahedral) are achievable. Thus, the aromatic structure found for (OBPMe)Pd^{II} does not result from the energetic preferences of the ligand but rather from the coordination of the palladium(II) ion.

22-Methylated Complexes. DFT Calculations. DFT calculations have also been carried out for (OBPMe)Pd^{II} and [(HOBPMe)Pd^{II}]$^+$. The optimized geometries of **5′** and **5′**-H$^+$ (with alkyl groups removed as before) are shown in Figure 6. The six-membered ring in **5′** is tipped out of the macrocyclic

(53) Ghosh, A.; Almlöf, J. *Chem. Phys. Lett.* **1993**, *213*, 519.
(54) Reimers, J. R.; Lü, T. X.; Crossley, M. J.; Hush, N. S. *J. Am. Chem. Soc.* **1995**, *117*, 2855.
(55) Hambright, P.; Chock, P. B. *J. Am. Chem. Soc.* **1974**, *96*, 3123.
(56) Longo, R. F.; Brown, E. M.; Quimby, D. J.; Adler, A. D.; Meot-Ner, M. *Ann. N.Y. Acad. Sci.* **1973**, *206*, 420.
(57) Longo, R. F.; Brown, E. M.; Rau, G. W.; Adler, A. D. In *The Porphyrins*; Dolphin, D., Ed.; Academic Press: New York, 1978; Vol. 5, p 459.
(58) Bain-Ackerman, M. J.; Lavallee, D. K. *Inorg. Chem.* **1979**, *18*, 3358.

Table 2. Bonding Distances and Their Mean Standard Deviations along the Three Possible Delocalization Pathways

	1′-*1*	**1′**-*4*	**1′**-*5*	**1′**-*6*	**5′**	**5**-H^+
C(6)−C(5)	1.409	1.444	1.373	1.401	1.391	1.424
C(21)−C(1)	1.411	1.444	1.363	1.394	1.382	1.420
C(1)−C(2)	1.504	1.426	1.495	1.419	1.508	1.430
C(2)−C(3)	1.465	1.398	1.465	1.399	1.458	1.407
C(3)−C(4)	1.351	1.383	1.356	1.388	1.365	1.392
C(4)−C(5)	1.457	1.416	1.439	1.404	1.453	1.421
C(1)−C(22)	1.399	1.407	1.507	1.522	1.496	1.479
C(22)−C(5)	1.409	1.407	1.505	1.516	1.494	1.476
$\sigma_{21-1-22-5-6}$ (**A**)	0.005	0.018	0.069	0.061	0.054	0.028
$\sigma_{1-2-3-4-5-22}$ (**B**)	0.050	0.014	0.053	0.056	0.048	0.033
$\sigma_{21-1-2-3-4-5-6}$ (**D**)	0.049	0.023	0.054	0.010	0.051	0.013

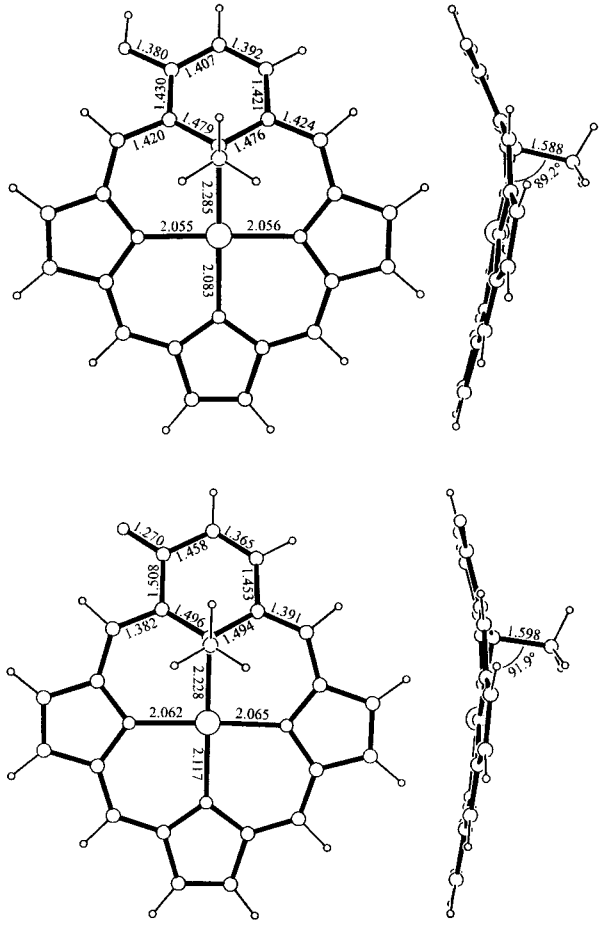

Figure 6. DFT-optimized structures of **5′** and **5′**-H^+ (selected bond distances in Å). Selected angles for **5′** (**5′**-H^+): C(1)−C(22)−Me 108.6° (111.8°), C(1)−C(22)−C(5) 113.8° (115.0°), C(5)−C(22)−Me 108.2° (111.3°), C(1)−C(22)−Pd 116.0° (113.2°), C(5)−C(22)−Pd 115.6° (113.6°), Pd−C(22)−Me 91.9° (89.2°). The interplanar angle between (C(1)C(2)C(3)C(4)C(5)C(22)) and (PdC(22)N(23)N(24)N(25)) is 25.0° (34.9°). Numbering of atoms corresponds to Chart 1.

plane by 25°. The methyl group is bound almost perpendicular to the CN_3 coordination square, and the C(22)−Me and C(22)−Pd bond distances are remarkably large.

In the calculated structure of **5′** one would expect delocalization modes **A** and **C** to be the main contributors, in proportions dependent on the nature of the C(22)−Pd interaction. (Structures **B** and **D** should be disfavored because of charge separation, Chart 2). Indeed, the external part of the six-membered ring shows an enone-type localization of bonds (O═C(2)−C(3)═C(4)), characteristic of both **A** and **C**. The C(1)−C(22) and C(5)−C(22) bonds, which belong to the inner part of the benzenoid ring, are very long (1.496, 1.494 Å, respectively), which is reflected by the high value of $\sigma_{21-1-22-5-6}$ (0.054). This corresponds to a nonplanar C(22) atom and the localized structure **C**. However, predominance of the **C** structure implies switching off the aromaticity of the system (both benzenoid and macrocyclic) and, as stated before, it contradicts the strong ring current observed for **5** in solution.

Two explanations of this discrepancy can be proposed. First, the electronic structure of **5** may easily be affected by hydrogen bonding to O(2) or interaction with solvent (through the Pd ion). The dominant form of **5** in solution may therefore differ from the isolated molecule used for calculations. On the other hand, the bond length criterion used here to assess aromaticity is not strictly applicable in the case of **5′** with a quadruply bound C(22). The C(1)−C(22) and C(5)−C(22) distances cannot be expected to approach the normal value for an "aromatic" C−C bond (∼1.40 Å) even when the three atoms are included in a delocalization pathway.

In the protonated form **5′**-H^+ the benzene ring is more tilted (35°), but angle Pd−C(22)−C(Me) is still close to 90°. The C(22) atom is now more pyramidal, the C−C(22)−C angles being in the range 111−115°. Notably, except for the degree of tilt of the six-membered ring the conformations of **5′**-H^+ and **1**-*6* are very similar. Bond averaging is more apparent than in **5′** and one might expect that **5′**-H^+ should be more aromatic. Bond length pattern in **5′**-H^+ most closely approaches delocalization mode **D**, although most of the pertinent distances are longer than expected.

The predictions of DFT methods correspond to the side-on coordination modes reported for *N*-alkyl porphyrins[44] and in particular for (21-CH_3CTPP)Ni^{II} and ((N_2CP-Tol)Pd^{II}.[7,25] In these complexes regular C-coordination is only possible with concomitant reduction of macrocyclic aromaticity and the observed geometry results from balancing two opposite effects. Van Koten's group provided an important precedent for this type of coordination.[43] In $[PtI((CH_3C_6H_3\text{-}(CH_2NMe_2)_2\text{-}o,o')]^+$ the Pt(II) ion was encapsulated by a pincer ligand and coordinated to the methylated carbon of the benzene ring (Pt−C = 2.183(7) Å). The environment of the coordinating carbon was slightly distorted toward pyramidal but the structural parameters and NMR data confirmed that the [6]annulene aromaticity was retained. In a later study Milstein and co-workers used a diphosphine pincer ligand to stabilize a η^2 agostic interaction between an arene C−H bond and rhodium(I).[59] The coordinated benzene ring remained aromatic, as evidenced by NMR and X-ray data, despite the strong interaction with the metal center.

Conclusions

In the present work we have described the synthesis and reactivity of K[(OBP)Pd^{II}], an organometallic complex of

(59) Vigalok, A.; Uzan, O.; Shimon, L. J. W.; Ben-David, Y.; Martin, J. M. L.; Milstein, D. *J. Am. Chem. Soc.* **1998**, *120*, 12539.

oxybenziporphyrin, showing that the ability of carbaporphyrinoids to coordinate metal ions and form metal−carbon bonds extends beyond the family of inverted porphyrin. The anionic $[(OBP)Pd^{II}]^-$ is conspicuous for the plasticity of its electronic structure, which is easily modified by addition of an electrophile. Depending on its nature, the electrophile reacts selectively at the O(2) atom (e.g. proton or acetyl) or is added to the internal carbon C(22) (methyl). O-addition results in structures with phenolic aromaticity, whereas the C(22)-substituted species retain their macrocyclic aromaticity despite the apparent interruption of the delocalization pathway by a pseudotetrahedral center. The internal alkylation is particularly important as it leads to a coordination mode that is drastically different from the in-plane coordination seen for $[(OBP)Pd^{II}]^-$.

The easy accessibility of the several delocalization patterns observed for oxybenziporphyrin and its complexes has been qualitatively explained through DFT studies. In most cases energy differences between possible tautomers of the free base are small suggesting that the π-electron density may be reorganized without significant destabilization of the molecule. This rationalizes the facile formation of oxybenziporphyrin complexes with both macrocyclic and phenolic aromaticity. Calculations carried out for the 22-substituted species predict a markedly distorted environment of the coordinating internal carbon leading to a structure that is difficult to describe in terms of a simple valence-bond model.

The coordinating environment provided by all carbaporphyrins offers a unique opportunity to create novel organometallic compounds and to control their reactivity. The additional feature of oxybenziporphyrin, its expanded π-system, has enabled us to investigate and eventually to control the subtle interplay between coordination, tautomerism, and aromaticity.

Experimental Section

Materials. 8,19-Dimethyl-9,13,14,18-tetraethyloxybenziporphyrin was synthesized as described before.[9,10] Solvents used in the syntheses were purified by standard methods. Deuterated solvents (CIL) were used as received, except for chloroform, which was deacidified by passing down a basic alumina column. Palladium chloride and trifluoroacetic acid (both from Aldrich) were used as received.

Instrumentation. NMR spectra were recorded at room temperature on a Bruker AMX 300 (^{1}H) and Bruker Avance 500 spectrometers (all heteronuclear experiments). Proton-detected ^{13}C and ^{15}N gradient-selected correlation spectra were measured using a 5 mm broad-band inverse gradient probehead. All 2D spectra were recorded with a resolution of 2048 data points in t_2 and up to 256 points in t_1 and processed in the standard way. The ^{1}H and ^{13}C shifts were referenced vs the residual solvent signal and the ^{15}N shifts vs neat nitromethane (external reference). Chemical shifts extracted directly from HMQC and HMBC maps are given without decimal digits. UV−vis spectra were recorded on a Hewlett-Packard 8435 diode-array spectrophotometer. The mass spectra were obtained on an AMD-604 spectrometer using EI and LSIMS ionization techniques or on a Finnigan MAT TSQ 700 spectrometer by means of the ESI method. The electrochemical measurements (MeCN, 0.1 M TBAP) were performed on an EA9C Multifunctional Electrochemical Analyzer using a glassy-carbon working electrode and platinum wire as the auxiliary electrode and referenced with a silver chloride electrode, which contacted the solution by a liquid junction.

K[(OBP)Pd^{II}]. A suspension of $(OBPH)H_2$ (20 mg, 42 μmol), $PdCl_2$ (7.5 mg, 42 μmol), and anhydrous K_2CO_3 (excess) in dry MeCN (40 mL) is refluxed for 5 h under nitrogen. The bright green solution is strongly concentrated (but not evaporated to dryness) and diluted with a small volume of CH_2Cl_2, and the complex is precipitated with hexane (recrystallization is repeated). The product is filtered out and dried overnight under vacuum. Yield: 25 mg (96%). ^{1}H NMR (MeCN-d_3): 10.37 (s, 21-H); 9.08 (s, 6-H); 9.22, 9.17 (2×s, 11,16-H); 8.62, 6.96 (AB, 4-H, 3-H, $^3J_{AB}$ = 8.8 Hz); ∼3.78 (m, 8 H, 9,13,14,18-α-Et); 3.32, 3.29 (2×s, 6 H, 8,19-Me); ∼1.75 (m, 12 H, 9,13,14,18-β-Et). ^{13}C NMR (partial data; $CDCl_3$, 4,7,13,16,21,24-hexaoxa-1,10-diazabicyclo[8.8.8]-hexacosane (Aldrich) added to improve solubility): 191 (2-C); 151 (4-C); 139 (22-C); 124 (3-C); 121 (6-C); 117 (21-C); 94, 95 (11,16-C); 20 (9,13,14,18-α-Et); 18 (9,13,14,18-β-Et); 11 (8,19-Me). ^{15}N NMR (same conditions as ^{13}C NMR): −212 (24-N); −225 (23-N); −226 (25-N); −352 (cryptate). UV−vis (MeCN, λ_{max} (nm) (log ϵ)): 443 (4.63), 338 (4.32), 601 (4.17), 588 (4.17), 642(3.98). HRMS (ESI, *m*/*z*, negative ions): 580.1604 (580.1587 for $C_{32}H_{32}N_3O^{106}Pd^-$).

(OBPMe)Pd^{II}. Solid **2** (5 mg) is placed in a small vial, and methyl iodide (1 mL) is added. The reaction mixture is stirred until the starting compound has dissolved. The brownish solution is evaporated in a stream of nitrogen and the residue dried under vacuum. The product does not require further purification. ^{1}H NMR ($CDCl_3$): 10.40 (s, 21-H); 9.25 (s, 6-H); 9.22, 9.20 (2 × s, 11,16-H); 9.10, 7.84 (AB, 4-H, 3-H, $^3J_{AB}$ = 9.3 Hz); ∼3.52 (m, 8 H, 9,13,14,18-α-Et); 3.09, 3.03 (2 × s, 6 H, 8,19-Me); ∼1.60 (m,12 H, 9,13,14,18-β-Et); −2.00 (s, 3 H, 22-Me). ^{13}C NMR ($CDCl_3$): 184.3 (2-C); 157.9 (1-C); 157.2 (5-C); 151.6, 150.1 (7-C, 20-C); 146.5 (×2, 9-C, 18-C); 145.4 (4-C); 143.6, 143.3 (×2), 143.1 (10-C, 12-C, 15-C, 17-C); 142.2, 142.1 (13-C, 14-C); 136.0, 134.7 (8-C, 19-C); 130.8 (3-C); 122.6 (6-C); 121.0 (21-C); 108.2, 108.0 (11-C, 16-C); 44.3 (22-C); 30.0 (22-Me); 19.4 (×2), 19.1 (×2) (9,13,14,18-α-Et); 18.0 (×2), 17.1 (×2) (9,13,14,18-β-Et); 11.4, 11.1 (8,19-Me). MS (ESI, *m*/*z*): 595.2 (595.18 calculated for $C_{33}H_{35}N_3O^{106}Pd^+$).

(OBP-*n*-Bu)Pd^{II} and (*n*-BuOBP)Pd^{II}. The synthesis is carried out analogously, *n*-BuI replacing methyl iodide. Gentle heating (50−60 °C, 1 h) is necessary to speed up the reaction. A mixture of the O- and C-substituted compounds **4**-Bu and **5**-Bu is obtained. Only **4**-Bu survives chromatographic workup (silica gel/CH_2Cl_2), and thus, **5**-Bu has only been characterized in the reaction mixture. Data for **4**-Bu are as follows. ^{1}H NMR ($CDCl_3$): 9.04 (s, 21-H); 7.82 (s, 6-H); 7.62 (s, 2 H, 11,16-H); 8.16, 7.20 (AB, 4-H, 3-H, $^3J_{AB}$ = 9.5 Hz); ∼3.10 (m, 8 H, 9,13,14,18-α-Et); 2.71, 2.70 (2 × s, 6 H, 8,19-Me); ∼1.44 (m,12 H, 9,13,14,18-β-Et); 4.38 (t, 2 H, 2-α-Bu); ∼2.06 (m, 2 H, 2-β-Bu); ∼1.74 (m, 2 H, 2-γ-Bu); 1.11 (t, 3 H, 2-δ-Bu). Data for **5**-Bu are as follows. ^{1}H NMR (MeCN-d_3, partial data): 10.25 (s, 21-H); 9.35 (s, 6-H); 9.25, 9.20 (2 × s, 11,16-H); 9.14, 7.56 (AB, 4-H, 3-H, $^3J_{AB}$ = 9.2 Hz); ∼2.40 (m, 2 H, 22-α-Bu).

(AcOBP)Pd and (TsOBP)Pd. Solid **2** (5 mg) is dissolved in a small volume of pyridine, and Ac_2O (4 μL, ∼5 equiv) or TsCl (3 mg, 2 equiv) is added. After 0.5 h of stirring, the solvent is removed in a stream of nitrogen. The residue is recrystallized from CH_2Cl_2/hexane. Data for **4**-Ac are as follows. ^{1}H NMR ($CDCl_3$): 8.03 (s, 21-H); 7.52 (s, 6-H); 7.24, 7.22 (2 × s, 11,16-H); 8.00, 7.37 (AB, 4-H, 3-H, $^3J_{AB}$ = 8.2 Hz); ∼2.93 (m, 8 H, 9,13,14,18-α-Et); 2.56, 2.54 (2 × s, 6 H, 8,19-Me); ∼1.37 (m,12 H, 9,13,14,18-β-Et); 2.54 (s, 3 H, 2-Ac). ^{13}C NMR ($CDCl_3$): 156 (2-C); 142 (4-C); 142 (22-C); 120 (3-C); 127 (6-C); 116 (21-C); 96, 95 (11,16-C); 21 (2-Ac); 19 (9,13,14,18-α-Et); 15, 16 (9,-13,14,18-β-Et); 10 (8,19-Me). Data for **4**-Ts are as follows. ^{1}H NMR ($CDCl_3$): 7.70 (s, 21-H); 7.41 (s, 6-H); 7.14, 7.10 (2 × s, 11,16-H); 7.91, 7.54 (AB, 4-H, 3-H, $^3J_{AB}$ = 8.3 Hz); ∼2.88 (m, 8 H, 9,13,14,-18-α-Et); 2.52, 2.25 (2 × s, 6 H, 8,19-Me); ∼1.31 (m,12 H, 9,13,14,-18-β-Et); 7.70, 7.14 (A_2B_2, 2-Ts, $^3J_{AB}$ = 8.2 Hz), 2.32 (s, 3 H, 2-Ts).

Calculation Method. The calculations were carried out with the GAUSSIAN94 program.[60] All structures were optimized within unconstrained C_1 symmetry of the system using the density functional theory (DFT) with Becke's three-parameter exchange functionals and the gradient-corrected functionals of Lee, Yang, and Parr (DFT(B3-LYP)).[61−64] The final estimations of the total energies were performed

(60) Frisch, M. J.; Trucks, G. W.; Schlegel, H. B.; Gill, P. M. W.; Johnson, B. G.; Robb, M. A.; Cheeseman, J. R.; Keith, T.; Petersson, G. A.; Montgomery, J. A.; Raghavachari, K.; Al-Laham, M. A.; Zakrzewski, V. G.; Ortiz, J. V.; Foresman, J. B.; Cioslowski, J.; Stefanov, B. B.; Nanayakkara, A.; Challacombe, M.; Peng, C. Y.; Ayala, P. Y.; Chen, W.; Wong, M. W.; Andres, J. L.; Replogle, E. S.; Gomperts, R.; Martin, R. L.; Fox, D. J.; Binkley, J. S.; Defrees, D. J.; Baker, J.; Stewart, J. P.; Head-Gordon, M.; Gonzales C.; Pople, J. A. *GAUSSIAN94*; Gaussian, Inc.: Pittsburgh, PA, 1995.
(61) Becke, A. D. *Phys. Rev. A* **1988**, *38*, 3098.

at the B3LYP level with the 6-31**G basis set (structures **1′**-*1*−*6*) or the LANL2DZ basis set (**5′** and **5′**-H^+) using the B3LYP/6-31*G fully optimized structures. The harmonic vibrational frequencies were calculated using analytical second derivatives and zero-point vibrational energies (ZPVE) were derived.

Acknowledgment. Financial support from the State Committee for Scientific Research KBN of Poland (Grant 3 T09A 155 15), the Foundation for Polish Science (M.S., L.S., and L.L.-G.), and the National Science Foundation (Grant CHE-9732054, T.L.) is kindly acknowledged. The quantum calculations have been carried out at the Poznań Supercomputer Center (Poznań) and the Wrocław Supercomputer Center (Wrocław).

(62) Lee, C.; Yang W.; Parr, R. G. *Phys. Rev. B* **1988**, *37*, 785.
(63) Johnson, B. G.; Gill, P. M. W.; Pople, J. A. *J. Chem. Phys.* **1993**, *98*, 5612.
(64) Becke, A. D. *J. Chem. Phys.* **1993**, *98*, 5648.

Supporting Information Available: Tables of total energies, bonding distances between heavy atoms, and optimized geometries (in *xyz* format) for structures **1′**-*1*−*6*, **5′**, and **5′**-H^+. This material is available free of charge via the Internet at http://pubs.acs.org.

IC010394A